

NIR spectrometry for the characterization of fuel components in a novel tamper-resistant pill bottle

Joseph P. Medendorp¹, Jason A. Fackler¹, Tom Henninger², Bill Dieter³, and Robert A. Lodder¹

¹Department of Pharmaceutical Sciences, College of Pharmacy, A123 ASTeCC Bldg. 0286, Lexington, KY 40536, USA

²Electrical and Computer Engineering, 683 Anderson Hall 0046, Lexington, KY, 40536, USA

³Center for Manufacturing, 413 Center for Robotics and Manufacturing Systems 0108, Lexington, KY 40536, USA

Corresponding author: Lodder, R.A. (lodder@uky.edu).

The purpose of this paper is twofold: (i) to present the Pill Safe, a novel design for a tamper-resistant prescription container, and (ii) to present use of near-infrared (NIR) spectrometry for characterization of fuel components and prediction of the burn characteristics of the fuel mixtures used to destroy tablets in the Pill Safe. In the safe, drug tablets are stacked next to fuel and attempts to force the mechanism or penetrate the bottle cause their instant destruction. The Pill Safe offers a second line of defense against the illicit distribution of dangerous prescription drugs.

Introduction

OxyContin, the brand name for the narcotic pain reliever Oxycodone-HCl (Purdue Pharma, <http://www.pharma.com/>), is categorized as a Schedule II drug under the Controlled Substances Act owing to its propensity for abuse and dependency [1]. It is an opium-based pain reliever prescribed for relief of moderate to severe pain; however, it exhibits heroin-like effects lasting up to 12 h when abused. The illicit diversion of pharmaceuticals such as OxyContin is a pervasive problem across the USA [2]. Measures have been implemented to protect pharmaceuticals and to prevent their illegal distribution. For example, electronically monitored narcotic cabinets and use of IDenticards (smart-card technology that can integrate electronic, magnetic stripe or barcode technologies, and biometric readers to increase security) have reduced diversion of drugs from hospitals and pharmacies. But it is now time for a second line of defense, in the form of well-secured, better-regulated pill dispensing

systems, to help prevent drug diversion from dispensed prescriptions. Companies have attempted to respond to this need, and e-pill (<http://www.epill.com/>) has developed a Monitored Automatic Pill Dispenser (MD.2; <http://www.epill.com/md2.html>) that features voice alarms and reminders. To our knowledge, the MD.2 is the only automated vault-like delivery system on the market. At a high retail price, the cost of dispensing new MD.2 bottles with each monthly refill would be prohibitive. Therefore, the MD.2 comes with a lock and key, and it is the responsibility of the patient to refill their bottles – potential thieves need only to obtain the key to pilfer the MD.2 contents. Thus, an opportunity lies in building an inexpensive and impenetrable container as a fail-safe, capable of scheduling and dispensing medications such as OxyContin, and deterring those interested in obtaining the drugs purely for abuse and illicit purposes.

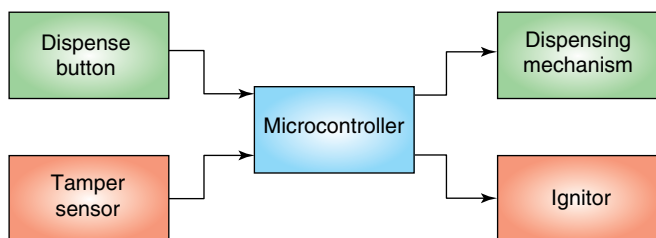


Figure 1. Schematic illustration of the main components of the medicine dispenser. A microcontroller serves as the master coordinator. Based on the inputs and programmed dispensing instructions, the microcontroller dispenses the tablet as needed. If the sensor is perturbed, the microcontroller signals for tablet neutralization, triggering the ignition of the fuel components.

Pill Safe

In response to the need for a better-protected pill bottle, the medicine dispenser presented in this research (conceived by RAMM, LLC, Bourbon County, KY USA) helps prevent the diversion of dangerous prescription drugs. The medicine dispenser simply presents the patient with a button. When

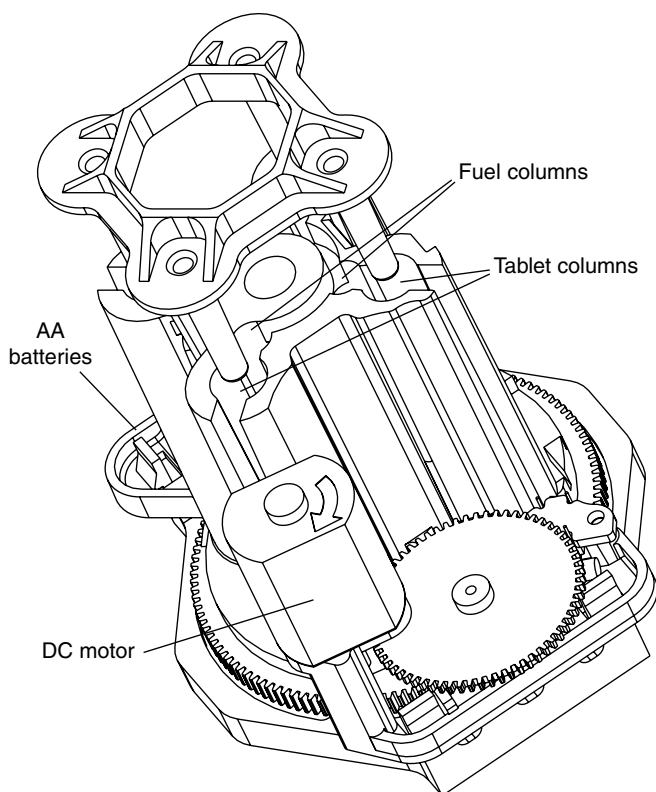


Figure 2. The medicine dispenser and its main components. Powered entirely by two AA batteries, the microcontroller activates the DC motor to dispense a tablet once per dosing period. A conductive loop wraps around the assembly. Disruption of this loop causes the microcontroller to ignite the fuel columns and incinerate the tablets. Fully assembled, the Pill Safe is 11.5 cm tall, 10 cm wide and 8.5 cm long.

pressed, it dispenses the medication through a small aperture if and only if the prescribed dosing period has passed since the previous pill was dispensed. Meanwhile, the medicine dispenser monitors its outer shell for tampering, rapidly destroying all of the pills contained within upon tamper detection. Destroying tablets rapidly requires a very fast, reliable chemical reaction that proceeds in the presence of interferences. Because the tablets are stored for an extended period in close proximity to the components of this reaction, the destructive reaction must not proceed even at a very low rate in the absence of a tampering trigger. For these reasons, a stable metallic aluminum-based fuel was chosen as the means of tablet destruction. Figure 1 gives a block diagram of the system; the mechanism shown in Figure 2 houses and delivers the pills and destroys them at the direction of the microcontroller. The pills are stored in columns adjacent to fuel. In this configuration, hot exhaust gases from the burning fuel are directed toward the pills. The entire assembly is essentially in a miniature vented Thermos® bottle, enveloped in a protective shell with a loop printed on the interior using conductive ink. Breaching the shell breaks the loop, signaling the microcontroller to ignite the fuel. The entire system is powered by two alkaline AA batteries and constructed from inexpensive parts, costing less than US \$10.

The medicine dispenser was designed to satisfy three main regulatory concerns: clinical, pharmaceutical, and packaging. From the clinical aspect, it was necessary that the burn residue from the incinerated medicine dispenser was completely destroyed and inedible. From the pharmaceutical aspect, drug tablets stacked next to fuel rods needed to be stable over time, not subject to chemical degradation in the presence of fuel. And lastly, the packaging for the medicine dispenser needed to be safe and inaccessible to those for whom the medicine is not intended. It also was designed so the hot gases created upon ignition are brief in duration and contained in an insulating vessel so there is no danger of igniting external fires.

Near-infrared (NIR) spectrometry was used in design of the fuel mixtures, for quantification of the fuel components, and for prediction of burn characteristics of the different fuel mixtures. Monitoring of fuel components using NIR is important because burn characteristics depend on the identity and quantity of fuel components (e.g., when the fuel mixture is deficient in ammonium perchlorate, the burn duration increases significantly, giving would-be thieves crucial extra seconds to break into the medicine dispenser). The fuel mixtures that were most effective in the Pill Safe were those that ignited the fastest and burned most completely. In these experiments, the concentrations were known before mixing the samples, but an in-process assay capable of assessing fuel mixtures would enable rapid and accurate detection of manufacturing and formulation inconsistencies.

Continued on page 56.

NIR has previously been used with great success for the quantification of fuel components in both solid and liquid propellant mixes [3,4]. NIR and Fourier transform infrared (FTIR) spectroscopy have been used for accurate and precise quality-control analysis of fuel pre-mixes, and have monitored antioxidant depletion over time [5]. In-process reaction information, such as intensity distribution, ignition processes, reaction temperatures, and the identity and concentrations of reaction species have been studied using the spectral range from UV and visible to NIR and mid-infrared [6]. Safety considerations for sample analysis using NIR for the study of fuel components, such as the thermal response to NIR exposure and the effects of Raman spectroscopy on the mixtures [7], also were addressed.

Theory

Absorbance in the NIR region of the electromagnetic spectrum is primarily a result of overtones and combinations of the fundamental bands from the mid-infrared and far-infrared regions. The bands are a result of anharmonic stretching and bending of functional groups such as N–H, O–H, C–H, and C=O. In most cases, the molecular structures are sufficiently complex that the spectral features of interest are highly overlapping, and thus, not directly usable without multivariate data analysis (Introduction to NIR Technology, Analytical Spectral Devices Inc., http://www.asdi.com/asd-600510_nir-introduction_rev.c.pdf). The formula for the medicine dispenser fuel source used to destroy pills included aluminum dust with iron oxide catalyst (fuel), NH₄ClO₄ (oxidizer), bisphenol A/epichlorohydrin (casting agent), and a polyamide resin (curing agent). The oxidizer, casting agent, and curing agent are the primary spectroscopically active constituents in this mixture; therefore, their concentrations were used for building and testing the regression model. Rather than using absolute mass, the prediction model used the constituent percentages (by mass) of the total mixture.

Because NIR spectra are usually a linear combination of pure component spectra, according to Beer's Law, it is theoretically possible to determine the concentration of each individual component in overlapping spectra. However, noise factors tend to complicate this procedure, such as sample inhomogeneity, particle size differences, and temperature drift. For a linear calibration model, outlying samples must be identified as outliers and removed from the calibration, or the noise and variation must be incorporated into the model. In this work, Hadi outlier detection was used to identify the spectra that belonged in the calibration model [8]. Outlier detection is generally approached by forming a clean subset of data **M** (free from outliers), followed by testing the fit of the remaining points relative to the clean subset. Consider the regression in Equation 1:

$$\mathbf{Y} = \mathbf{X}\boldsymbol{\beta} + \boldsymbol{\epsilon} \tag{Eqn 1}$$

where **Y** is an $n \times 1$ vector of responses, **X** is an $n \times k$ matrix of responses and observations, **β** is a vector of estimated regression coefficients from fitting the model to **M**, and **ε** is a matrix of errors. The best clean subset **M** is found by the deletion of the variables that result in the largest reduction in the residual sum of squares (SSE_M).

When building a calibration model from NIR spectra, it can be helpful to visualize the total instrument response, **r_k**, as the sum of two orthogonal components: the interferences, **r_k[−]**, and the net analyte signal (NAS), **r_k[⊥]**, according to Equation 2 [9]. The superscript '−' denotes the fact that the interferences span the space occupied by the analyte, and the '⊥' denotes the fact that the NAS is orthogonal to the interfering species.

$$\mathbf{r}_k = \mathbf{r}_k^- + \mathbf{r}_k^\perp \tag{Eqn 2}$$

A linear combination of the interferences produces **r_k[−]**; therefore, the signal orthogonal to **r_k[−]** belongs exclusively to the analyte of interest [10]. A projection matrix is calculated according to Equation 3:

$$\mathbf{P}_k^\perp = (\mathbf{I} - \mathbf{R}_{-k}\mathbf{R}_{-k}^+)$$
(Eqn 3)

where **R_{-k}** is a matrix of samples without the analyte, **I** is the identity matrix, and the superscript '+' is the Moore–Penrose pseudoinverse. The NAS vector, **r_{cal}[⊥]**, can be calculated from a calibration spectrum, **r_{cal}**, by projection of the spectrum onto the null space of the rows of **R** with Equation 4:

$$\mathbf{r}_{cal}^\perp = \mathbf{P}_k^\perp \mathbf{r}_{cal} \tag{Eqn 4}$$

The NAS vector is normalized to length one by Equation 5:

$$\mathbf{r}_k^{NAS} = \frac{\mathbf{r}_{cal}^\perp}{\|\mathbf{r}_{cal}^\perp\|} \tag{Eqn 5}$$

A linear regression is fit to this vector, and the regression coefficients are used for subsequent predictions.

One advantage of using the NAS approach is in the calculation of so-called figures of merit. In severely overlapping spectra, it has historically been difficult to quantify selectivity, sensitivity, and signal-to-noise (S/N) ratio because of the inability to distinguish between interferences and the analyte of interest [10,11]. With the NAS, these quantities can be measured directly. Selectivity can be calculated as the scalar degree of overlap, *a*, between the NAS vector and the calibration spectrum according to Equation 6:

$$\alpha = \frac{\|\mathbf{r}_{cal}^\perp\|}{\|\mathbf{r}_{cal}\|} \quad (\text{Eqn 6})$$

The selectivity is a measure from 0 to 1 indicating how unique the analyte of interest is compared with the interferences. The sensitivity is a measure of how much the analyte varies in response to a change in concentration. This quantity can be expressed as Equation 7:

$$\mathbf{s}_k = \mathbf{r}_k^{NAS} / c_k \quad (\text{Eqn 7})$$

where c_k is the concentration of the k -th analyte. Theoretically, sensitivity should be the same for each concentration and each NAS vector [12]. The S/N ratio can be expressed as Equation 8:

$$S/N = \frac{c_k \|\mathbf{r}_k^{NAS}\|}{\|\boldsymbol{\epsilon}\|} \quad (\text{Eqn 8})$$

where $\boldsymbol{\epsilon}$ is the random instrumental error.

To prove that the relationship between NIR spectra and the fuel components is not a product of correlated initial constituent concentrations, the mixture concentrations were calculated by the following orthogonalization procedure. A random matrix \mathbf{A} corresponding to I mixtures and J components per mixture was constructed with a random-number generator. Singular value decomposition of \mathbf{A} according to Equation 9 yields orthogonal principal component scores, \mathbf{U} , between -1 and $+1$; \mathbf{S} is a diagonal matrix of singular values and \mathbf{V} is the matrix of eigenvectors (loadings) [13].

$$\mathbf{A} = \mathbf{USV} \quad (\text{Eqn 9})$$

A coefficient matrix, \mathbf{K} , was constructed according to Equation 10 such that each row contains 0 and 1.

$$\mathbf{K} = \frac{\min[\mathbf{U}_i] + [\mathbf{U}_i]_{j=1}^j}{\max[\mathbf{U}_i]} \quad (\text{Eqn 10})$$

A final matrix of concentrations was constructed by multiplication of \mathbf{K} with the fuel ratios from the accepted fuel formula [16% Atomized aluminum powder (fuel), 69.8% ammonium perchlorate (oxidizer), 0.2% iron oxide powder (catalyst), 12% binder, and 2% epoxy curing agent; http://www.nasa.gov/returntoflight/system/system_SRB.html].

In a search for the most descriptive multivariate model to correlate NIR spectra to constituent concentrations and burn characteristics, the present research compared NAS regression with principal component regression (PCR) [14], interval PCR (iPCR), and PCR-uninformative variable elimination (PCR-UVE) [15,16]. For each of these models, principal components were calculated by a singular value decomposition of the raw spectra according to Equation 9.

The regression of \mathbf{U} in Equation 11 indicates which of the components have the strongest correlation to a change in constituent concentration \mathbf{c} , where \mathbf{a} is the y -intercept, \mathbf{b} is a vector of regression coefficients, and $\boldsymbol{\epsilon}$ is the residual.

$$\mathbf{c} = \mathbf{a} + \mathbf{bU} + \boldsymbol{\epsilon} \quad (\text{Eqn 11})$$

Equation 12 demonstrates how a leave-one-out cross validation was used to predict the concentration of fuel components, where σ^2 is the variance, $f_i(\mathbf{U}_i)$ is the prediction of the model for the i -th pattern m in the training set, after it has been trained on the $m-1$ other patterns.

$$\sigma_{LOO}^2 = \frac{1}{m} \sum_{i=1}^{i=m} (\mathbf{c}_i - f_i(\mathbf{U}_i))^2 \quad (\text{Eqn 12})$$

Mixture	Al (%)	NH ₄ ClO ₄ (%)	Fe ₂ O ₃ (%)	Epoxy resin (%)	Curing agent (%)	Ignition time(s)	Burn duration(s)
1	13.34	58.03	0.37	21.46	6.81	2.0	14.0
2	10.02	60.52	0.40	21.09	7.97	1.5	11.0
3	16.69	60.47	0.51	16.96	5.36	2.0	15.0
4	9.40	69.57	0.33	15.46	5.24	0.5	9.0
5	19.23	51.70	0.55	21.53	7.00	4.0	18.0
6	17.07	44.82	0.45	28.06	9.59	3.5	26.0
7	21.33	36.64	0.39	31.31	10.33	4.0	40.0
8	13.13	56.60	0.24	22.89	7.14	2.0	16.0
9	16.65	69.92	0.27	9.83	3.33	1.0	6.0
10	12.38	63.17	0.29	18.22	5.93	1.5	12.0
11	11.02	59.31	0.41	20.06	9.2	1.5	4.0

Table 1. Constituent percentages, ignition time, and burn duration for each fuel mixture.

Continued on page 58.

NIR performance	NH ₄ ClO ₄		Epoxy resin		Curing agent		Ignition time		Burn duration	
	iPCR	NAS	iPCR	NAS	iPCR	NAS	iPCR	NAS	iPCR	NAS
r ²	0.992	0.983	0.969	0.997	0.987	0.996	0.959	0.993	0.917	0.989
RMSECV (%)	2.58	4.54	4.33	2.31	2.94	4.27	5.93	2.20	6.98	2.60
Position (nm) ^b	1566–1966		1324–1724		1633–2033		1750–2150		2088–2488	

^aNIR performance as values of r² and root-mean-square error of cross-validation (RMSECV) were predicted using interval principal component regression (iPCR) and net analyte signal (NAS).

^bThe wavelength regions were selected and used with iPCR, whereas NAS used the full spectrum.

Table 2. Predicted results for NH₄ClO₄, epoxy resin, curing agent, ignition times, and burn durations.^a

In the case of a two-component system, it is a simple matter to observe a linear change in the analyte concentration. In the presence of two system components, theoretically, the concentration change can be modeled by one principal component. The loading corresponding to this principal component accurately reflects the contribution of each wavelength to the overall classification. However, when multiple system components change simultaneously, multiple principal components are needed for the prediction model.

Interval PCR performs in similar way to the aforementioned analysis, but rather than using the full spectrum, it uses smaller subsets of variables [16]. For example, when the experimenter specifies an interval (I_n) of 100 wavelengths, the algorithm performs PCR followed by principal component selection and cross-validation on intervals of 100. With a moving boxcar, all wavelengths are paired with all other wavelengths inside of ±I_n. For example, after the algorithm analyzes 2101–2200 nm, the next iteration analyzes 2102–2201 nm, and so on. At the final wavelength, the first I_n wavelengths are added to the end for the final iterations. In this manner, each wavelength is included in a new model 2 × I_n times. The goal of interval selection is the minimization of the standard error of performance in Equation 13,

which indicates the interval with the highest correlation to the change in drug concentration:

$$SEP = \frac{\left(\frac{\epsilon^2}{N - 1} \right)^{1/2}}{\max(\mathbf{c}) - \min(\mathbf{c})} \quad (\text{Eqn 13})$$

where ϵ is the residual, N is the number of spectra, and \mathbf{c} is a concentration vector.

Experimental methods

Fuel preparation

Eleven different mixtures of ammonium perchlorate (NH₄ClO₄), aluminum dust (Al), iron oxide (Fe₂O₃), casting resin (Bisphenol A/Epichlorohydrin), and polyamide curing agent (Versamid 140; Firefox Enterprises, <http://www.firefox-fx.com/>) were constructed such that the percentage of each component did not correlate with those of the other components. Of the 11 fuel mixtures used, NH₄ClO₄ was 36.64 to 69.92% of the total mixture weight, Al was 9.40 to 21.33%, Fe₂O₃ was 0.24 to 0.51%, casting resin was 9.83 to 31.31%, and curing agent was 3.33 to 10.33%. Con-

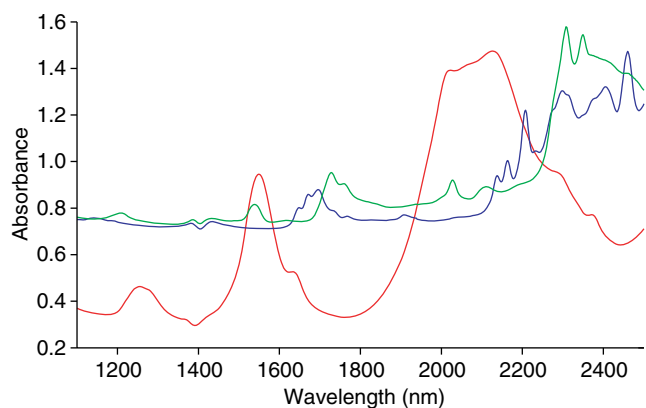


Figure 3. Pure-component NIR spectra. The spectrum for epoxy resin is in blue, that for curing agent is in green, and that for NH₄ClO₄ is in red.

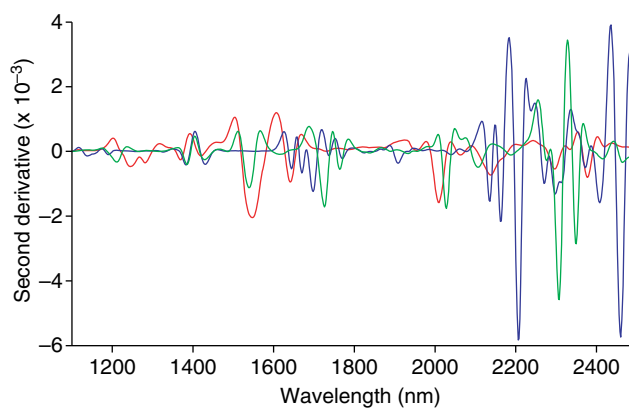


Figure 4. Second-derivative NIR spectra. The spectrum for epoxy resin is in blue, that for curing agent is in green, and that for NH₄ClO₄ is in red.

stituent ratios are reported in Table 1. Epoxy resin and curing agent were heated to 35°C on a hot plate. Powders were mixed together and stirred to ensure a homogenous mixture. Epoxy resin and curing agents were then added to the powder mixtures and stirred vigorously for three minutes. The resulting fuel was poured into a ceramic mold so it could easily be inserted into the medicine dispenser prototype.

NIR data collection

NIR spectra were collected in reflectance mode from 1100 to 2500 nm in 2 nm steps using a customized scanning spectrometer, as described previously [17]. To eliminate room noise, samples were scanned inside the instrument drawer. Each of the mixtures was scanned six times, all in random order to eliminate the effects of drift. All NIR data were exported to Matlab 7.0.1 (The Mathworks Company, <http://www.mathworks.com/>) for processing and analysis.

Ignition tests

To identify the burn characteristics, fuel samples were ignited quickly using a propane torch. With the torch and samples positioned reproducibly, ignitions were recorded on digital video and ignition start times and durations were noted (Table 1).

Analysis of NIR spectra

Algorithms for NAS, Hadi outlier detection, PCR, and iPCR were all written by the authors for Matlab 7.0.1. NAS, PCR, and iPCR were all used to predict the concentrations of each fuel component from the collected NIR spectra. These methods enabled the identification of the statistically significant regions of the NIR spectrum for the measurement of each component. Using the same methods, NIR spectra were then used to predict the ignition times and burn durations. The two most effective methods for calibration and prediction of burn characteristics were iPCR and NAS.

Extent of incineration

The extent of OxyContin incineration was determined by high-performance liquid chromatography (HPLC). The pill bottle was loaded with fuel mixture number 1 (Table 1). Burn residue from the pill bottle stacked with 20 mg OxyContin tablets (Purdue Pharma, <http://www.pharma.com/>) was ground with a mortar and pestle, washed with 200 ml of mobile phase, filtered twice through a 0.2 µm filter, and a chromatogram was collected to measure the remaining concentration of OxyContin. The HPLC assay was conducted using a Waters 717plus Autosampler, Waters 1525 Pump, and Waters 2487 Dual Wavelength Absorbance Detector with Waters Breeze v3.30 Software (<http://www.waters.com/>).

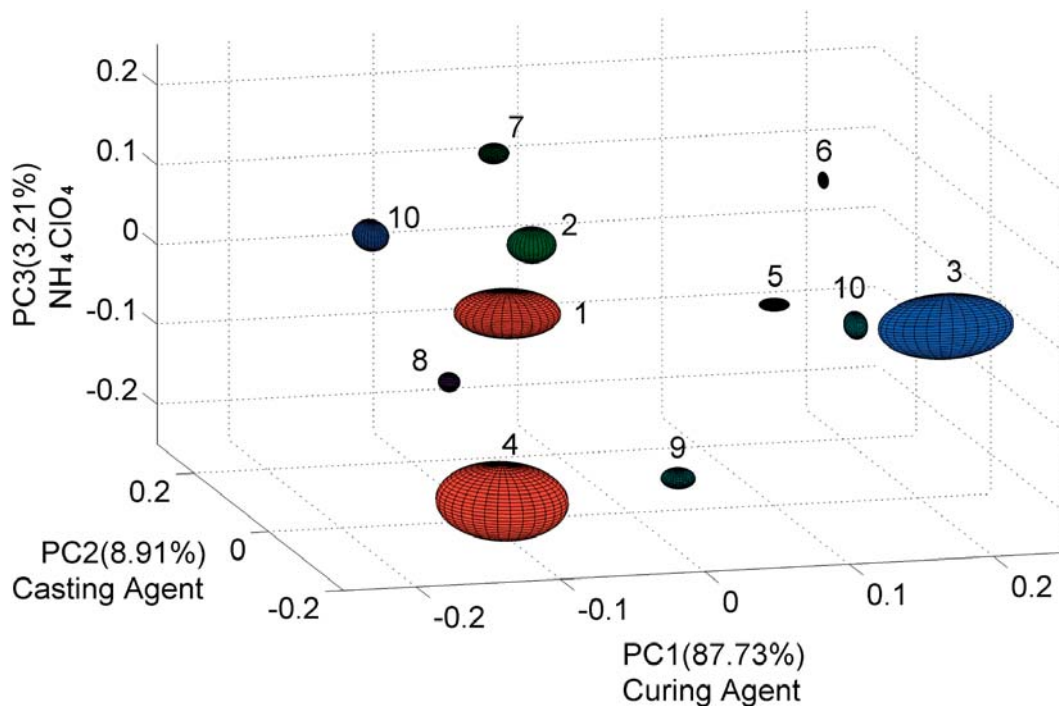


Figure 5. A plot of principal component (PC) scores indicates whether a mixture is deficient in a particular fuel component. PC score 1 correlates very highly with the presence of curing agent, PC2 with the presence of epoxy resin, and PC3 with the presence of NH_4ClO_4 . The mixture with ideal burn (fastest ignition and longest burn) was mixture number 1; therefore, projection of PC scores onto this plot can be used as a map for the prediction of fuel burn characteristics.

Continued on page 60.

A Waters μ Bondapak C18 column (300×3.9 mm) was used with the UV/VIS Detector set at a wavelength of 206 nm for OxyContin standards. The mobile phase used for OxyContin was 0.005 M 1-hexanesulfonate, methanol, phosphoric acid, and triethylamine (900:100:5:2). The flow rate of the mobile phase was at 1.5 ml min^{-1} with 10 ml injections of the sample. Standards analyzed exhibited excellent linearity over the concentration range employed. The retention time for OxyContin was 22.22 ± 0.211 min. The sensitivity of the assay was 25 ng ml^{-1} .

Results and discussion

HPLC analysis indicated that following tablet incineration using the most effective fuel mixture, the burn residue contained 5.58% by mass of the initial OxyContin. It must be noted that this 5.58% was recovered only by grinding, washing, extracting, filtering, purifying, and chromatographically separating the burn residue. With such an extensive extraction procedure and such a small yield, it is likely that would-be thieves would be sufficiently discouraged from a recovery attempt. The best fuel mixture required ~ 14 s to consume the contents of the safe completely, making it nearly impossible to break into the bottle and remove the contents before the burn was complete. The medicine dispenser is designed so that the flame is contained, and there is no danger of igniting external fires. The fuel formula contains an oxidizer; therefore, there is no need for atmospheric oxygen to sustain the reaction that destroys the tablets.

The most effective chemometric methods for the measurement of fuel components and prediction of ignition characteristics from the NIR spectra were NAS regression and iPCR. The fuel components had no significant correlation to each other; therefore, the predictive ability of the NIR was not a product of correlated concentrations. Additionally, the NAS was able to detect the portion of the signal that was unique to the analyte of interest; thus, there were two measures of certainty that the strong correlation was not an artifact. Using NAS, the NIR measurements over the respective concentration ranges resulted in $r^2 = 0.983$ and root-mean-square error of cross-validation (RMSECV) = 4.54% for NH_4ClO_4 , $r^2 = 0.997$ and RMSECV = 2.31% for the epoxy resin, and $r^2 = 0.996$ and RMSECV = 4.27% for the curing agent. NAS predicted ignition times with $r^2 = 0.993$ and RMSECV = 2.20% and burn durations with $r^2 = 0.989$ and RMSECV = 2.60%. Because this experiment was performed using cross validation, no external validation set was used. Consequently, all spectra satisfied the Hadi criterion for class membership; therefore, no spectra were discarded as outliers in the NAS calibration. The NAS calibration and figures of merit were calculated from the unsmoothed, unprocessed full spectrum data. Interval PCR data performed comparably to NAS data for the measurement of fuel concentrations, but not as well for the prediction of burn char-

acteristics. See Table 2 for comparison of iPCR and NAS performance statistics.

Pure-component and second-derivative NIR spectra from NH_4ClO_4 , epoxy resin, and curing agent are shown in Figures 3 and 4. It is apparent from these figures that the spectra were sufficiently distinct from each other, making it relatively easy to identify the NAS for each component. Iron oxide and aluminum had no distinguishing spectral features in the NIR; therefore, they were not quantified in this experiment. Of course, other fuel formulas could be used. A mixture with five components, each with its own unique NIR chromophore, might make the most sense from a quality-control standpoint. However, iron oxide can be determined in mixtures of aluminum dust using visible light spectrometry. Many NIR spectrometers are capable of collecting visible and NIR spectra simultaneously.

The figures of merit calculated from the NAS vector resulted in: selectivity = 0.014, sensitivity = 5.874, and S/N = 39.941 for NH_4ClO_4 ; selectivity = 0.005, sensitivity = 6.467, and S/N = 50.76 for the casting agent; and selectivity = 0.022, sensitivity = 4.097, and S/N = 35.32 for the curing agent. Selectivity is a unitless quantity, and sensitivity is given in units of signal per concentration. The limit of detection (LOD) is defined as the concentration at which S/N = 3 [10]. The S/N ratios were calculated separately for each individual concentration, and the theoretical LOD was extrapolated from the linear plot of concentration versus S/N. The LOD was 0.93% for NH_4ClO_4 , 1.37% for casting agent, and 1.36% for curing agent. Precision was measured by calculating the relative standard deviation (RSD) of the predicted concentrations from the NAS vector. The RSD was 0.38% for NH_4ClO_4 , 0.32% for casting agent and 0.70% for curing agent. Bias was calculated by subtraction of the measured NIR values from the reference gravimetric values. Although some of the individual measurements were offset slightly high or slightly low, there was no net bias for the calibration.

Figure 5 is a plot of principal component ellipses calculated from the fuel mixtures, demonstrating how well NIR was able to separate them. Ellipses are drawn six standard deviations from their cluster centers. NH_4ClO_4 demonstrated a high correlation to both ignition time and burn duration, suggesting that it was largely responsible for the reaction rates. High correlations were demonstrated by principal component (PC1) to the concentration of curing agent, PC2 to the concentration of casting agent, and PC3 to concentration of NH_4ClO_4 . Mixture 1 demonstrated the best burn characteristics for the purpose of this research (i.e., fastest ignition and longest burn). The cluster location from mixture 1 can quickly be compared with other fuel mixtures, enabling this figure to act as a map to identify components in which a particular mixture might be deficient. This figure also can be used to predict the ignition time and burn duration of each mixture depending on its constituent concentrations.

NIR spectroscopy is a versatile, nondestructive, and rapid method of analysis. It has been applied to both liquid and solid propellants with no sample preparation required [3–6]. As is evident from the PC clusters in Figure 5, it is also highly reproducible. Even when samples are very close to each other in concentration, they still cluster in distinctly different regions of a PC plot. This effect can be quantified by the bootstrap error-adjusted single-sample technique (BEST) [16]. According to the BEST, multidimensional standard deviations (MSD) greater than three indicate that clusters belong to different populations. When MSDs are less than three, clusters are considered inseparable. The average MSD separation between fuel mixtures was 431.36, and the average MSD separation calculated between repeat scans of the same mixture was 1.69, demonstrating the high degree of reproducibility from scan to scan. NIR analysis is also a rapid technique. NIR spectrometers can now collect thousands of spectra per second with high resolution [18], and NIR can effectively function as an in-process assay for the quantification of fuel mixtures as they are cast into the medicine dispenser model. From the 200 NIR spectra collected for this experiment, there were no aberrant scans, demonstrating that NIR is also a robust assay.

Conclusion

This research presents a novel design for a medicine dispenser, intended to provide a second line of defense against the diversion of prescription drugs. NIR spectroscopy was able to quantify rapidly and accurately the fuel components in solid fuel mixtures, and to identify burn characteristics of the different mixtures. This research suggests that Pill Safe manufacturing and the fuel analysis need not be too challenging or expensive, making it a valuable product for use in the pharmaceutical industry.

Acknowledgements

This research was supported in part by the US FDA through contract 200406251503 and through KSEF-148–502–03–61.

References

1. National Drug Intelligence Center (2002) *Information Brief: Prescription Drug Abuse and Youth*. (<http://www.usdoj.gov/ndic/pubs1/1765>).
2. The New York Times (2004) Pill thefts alter the look of rural drugstores. *The New York Times* (<http://query.nytimes.com/gst/health/article-page.html?res=9C03E1D6163BF935A35754C0A9629C8B63>).
3. Wang, J. *et al.* (2004) Application of near infrared spectroscopy in liquid propellant analysis. *Huaxue Tongbao* 67, w023/1–w023/4.
4. Judge, M.D. (2004) The application of near-infrared spectroscopy for the quality control analysis of rocket propellant fuel pre-mixes. *Talanta* 62, 675–679.
5. Rohe, T. *et al.* (1996) Near infrared-transmission spectroscopy on propellants and explosives. *Int. Annu. Conf. ICT* 27, 85.1–85.10 (<http://www.ict.fraunhofer.de/english/events/anconf/a27general.html>).
6. Weiser, V. and Eisenreich, N. (2005) Fast emission spectroscopy for a better understanding of pyrotechnic combustion behavior. *Propellants Explos. Pyrotech.* 30, 67–78.
7. Harvey, S.D. *et al.* (2003) Safety considerations for sample analysis using a near-infrared (785 nm) Raman laser source. *App. Spec.* 57, 580–587.
8. Hadi, A.S. and Simonoff, J.S. (1993) Procedures for the identification of multiple outliers in linear models. *J. Am. Stat. Assoc.* 88, 1264–1272.
9. Boelens, H.F. *et al.* (2004) Performance optimization of spectroscopic process analyzers. *Anal. Chem.* 76, 2656–2663.
10. Lorber, A. (1986) Error Propagation and figures of merit for quantification by solving matrix equations. *Anal. Chem.* 58, 1167–1172.
11. Booksh, K.S. and Kowalski, B.R. (1994) Theory of analytical chemistry. *Anal. Chem.* 66, 782a–791a.
12. Lorber, A. *et al.* (1997) Net analyte signal calculation in multivariate calibration. *Anal. Chem.* 69, 1620–1626.
13. Jolliffe, I.T. (2002) *Principal Component Analysis*. Springer.
14. Leardi, R. and Norgaard, L. (2004) Sequential application of backward interval partial least squares and genetic algorithms for the selection of relevant spectra regions. *J. Chemometr.* 18, 486–497.
15. Noord, O.E. (1996) Elimination of uninformative variables for multivariate calibration. *Anal. Chem.* 68, 3851–3858.
16. Lodder, R.A. and Hieftje, G. (1988) Detection of subpopulations in near-infrared reflectance analysis. *App Spec.* 42, 1500–1512.
17. Yokel, R.A., *et al.* (2005) ²⁶Al-containing acidic and basic sodium aluminum phosphate preparation and use in studies of oral aluminum bioavailability from foods utilizing ²⁶Al as an aluminum tracer. *Nucl. Instrum. Methods Phys. Res. B* 229, 471–478.
18. Klahn, T. *et al.* (2004) A high speed NIR-spectroscopy to investigate ignition and combustion of propellants and pyrotechnics. *Int. Annu. Conf. ICT* 35, 161/1–161/9 (http://www.ict.fraunhofer.de/english/presse/anre2004_05.pdf). 